

Proceedings of the  
9th International Conference on  
Climbing and Walking Robots

**CLAWAR  
2006**

12-14 September 2006, Brussels, Belgium

Edited by Yvan Baudoin & Dirk Lefeber



# Comparison of Different Fractional Order PD<sup>0.5</sup> Control Algorithm Implementations for Legged Robots

Manuel F. Silva, J. A. Tenreiro Machado, Ramiro S. Barbosa  
Department of Electrical Engineering, Institute of Engineering of Porto,  
Rua Dr. António Bernardino de Almeida – 4200-072 Porto – Portugal  
email: mss@isep.ipp.pt, jtm@isep.ipp.pt, rsb@isep.ipp.pt

**Abstract:** This paper studies different Fractional Order (FO) PD<sup>0.5</sup> algorithms applied to the leg joint control of a hexapod robot with two dof legs. For the implementation of the FO PD<sup>0.5</sup> joint controllers both the Padé and the series approximations are considered, being compared their performance. For simulation purposes the robot prescribed motion is characterized through several locomotion variables and parameters and for the walking performance evaluation two indices are used, one of them based on the mean absolute density of energy per travelled distance and the other one on the hip trajectory errors. A set of simulation experiments reveals the influence of the different approximations and the order of the PD<sup>0.5</sup> controllers tuning upon the proposed indices.

**Keywords:** Robotics, Locomotion, Control algorithms, Fractional-order control, Performance analysis

## I. INTRODUCTION

Legged robots allow locomotion in terrain inaccessible to other type of vehicles, but the requirements for leg coordination and control impose difficulties beyond those encountered in wheeled robots. Previous studies focused mainly in the control at the leg level and leg coordination using different methods. In spite of the diversity of approaches, for multi-legged robots the control at the joint level is usually implemented through a simple PID like scheme with position / velocity feedback [1]. Other approaches include sliding mode control, computed torque control and hybrid force / position control [1].

The application of the theory of fractional calculus in robotics is still in a research stage, but the recent progress in this area reveals promising aspects for future developments [1]. Besides, FO controllers often achieve better performance and robustness results when compared with integer order ones, particularly when the system under control presents fractional dynamics, as seems to be this case [2].

Taking into consideration these facts, a simulation model for multi-leg locomotion systems was developed, for several periodic gaits, and for its control we adopt a cascade control architecture with two controllers  $G_{c1}(s)$  and  $G_{c2}$  in the forward control path. In the present study we consider a FO PD<sup>0.5</sup> algorithm for  $G_{c1}(s)$ , and evaluate and compare the performance of two distinct alternatives for implementing the FO algorithm, namely a discrete-time  $u^{\text{th}}$  order Padé approximation and a truncated series of  $v$  terms. The analysis is based on the formulation of two indices measuring the mean absolute density of energy per travelled distance and the hip trajectory errors during walking.

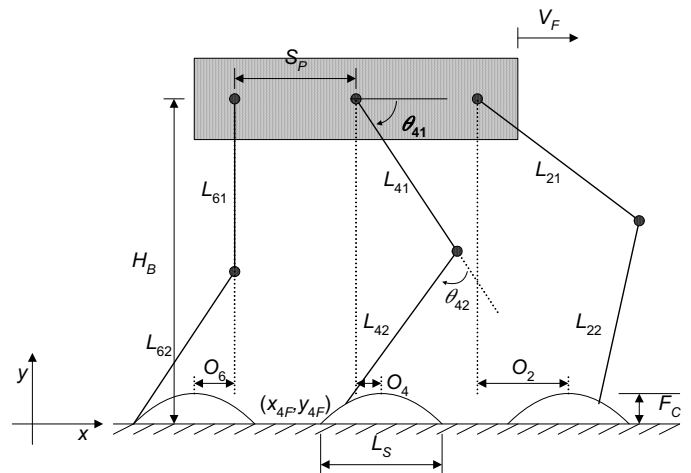


Fig. 1. Coordinate system and variables that characterize the motion trajectories of the multi-legged robot.

Bearing these facts in mind, the paper is organized as follows. Section two introduces the robot kinematics and the motion planning scheme. Sections three and four present the robot dynamic model and control architecture, and the optimizing indices, respectively. Section five develops a set of simulation experiments to compare the performance of the different PD<sup>0.5</sup> control algorithms implementation when applied to the hexapod joint leg control. Finally, section six outlines the main conclusions and some directions towards future developments.

## II. ROBOT KINEMATICS AND TRAJECTORY PLANNING

We consider a walking system (Fig. 1) with  $n=6$  legs, equally distributed along both sides of the robot body, having each two rotational joints (*i.e.*,  $j = \{1, 2\} \equiv \{\text{hip, knee}\}$ ) [3].

Motion is described by means of a world coordinate system. The kinematic model comprises: the cycle time  $T$ , the duty factor  $\beta$ , the transference time  $t_T = (1-\beta)T$ , the support time  $t_S = \beta T$ , the step length  $L_S$ , the stroke pitch  $S_p$ , the body height  $H_B$ , the maximum foot clearance  $F_C$ , the  $i^{\text{th}}$  leg lengths  $L_{i1}$  and  $L_{i2}$  and the  $i^{\text{th}}$  foot trajectory offset  $O_i$ . Moreover, we consider a periodic trajectory for each foot, with body velocity  $V_F = L_S / T$ .

Gaits describe sequences of leg movements, alternating between transfer and support phases. Given a particular gait and duty factor  $\beta$ , it is possible to calculate, for leg  $i$ , the corresponding phase  $\phi_i$ , the time instant where each leg leaves and returns to contact with the ground and the cartesian trajectories of the tip of the feet (that must be completed

during  $t_T$ ). Based on this data, the trajectory generator is responsible for producing a motion that synchronises and coordinates the legs.

The robot body, and by consequence the legs hips, is assumed to have a desired horizontal movement with a constant forward speed  $V_F$ . Therefore, for leg  $i$  the cartesian coordinates of the hip of the legs are given by  $\mathbf{p}_{Hd}(t) = [x_{iHd}(t), y_{iHd}(t)]^T$ :

$$\mathbf{p}_{Hd}(t) = [V_F t + Sp(1 - \text{ceil}(i/2)) \quad H_B]^T \quad (1)$$

Regarding the feet trajectories, on a previous work we evaluated two alternative space-time foot trajectories, namely a cycloidal and a sinusoidal function [4]. It was demonstrated that the cycloid is superior to the sinusoidal function, since it improves the hip and foot trajectory tracking, while minimising the corresponding joint torques. However, a step acceleration profile is assumed for the feet trajectories. These results do not present significant changes for different acceleration profiles of the foot trajectory.

In order to avoid the impact and friction effects, at the planning phase we impose null velocities of the feet in the instants of landing and taking off, assuring also the velocity continuity.

Considering the above conclusions, for each cycle the desired geometric trajectory of the foot of the swing leg is computed through a cycloid function (Eq. 2). For example, considering that the transfer phase starts at  $t = 0$  s for leg  $i = 1$  we have for  $\mathbf{p}_{Fd}(t) = [x_{iFd}(t), y_{iFd}(t)]^T$ :

- during the transfer phase:

$$\mathbf{p}_{Fd}(t) = \left[ V_F \left[ t - \frac{t_T}{2\pi} \sin\left(\frac{2\pi t}{t_T}\right) \right], \frac{F_C}{2} \left[ 1 - \cos\left(\frac{2\pi t}{t_T}\right) \right] \right]^T \quad (2)$$

- during the stance phase:

$$\mathbf{p}_{Fd}(t) = [V_F T \quad 0]^T \quad (3)$$

The algorithm for the forward motion planning accepts the desired cartesian trajectories of the leg hips  $\mathbf{p}_{Hd}(t)$  and feet  $\mathbf{p}_{Fd}(t)$  as inputs and, by means of an inverse kinematics algorithm  $\Psi^{-1}$ , generates the related joint trajectories  $\Theta_d(t) = [\theta_{i1d}(t), \theta_{i2d}(t)]^T$ , selecting the solution corresponding to a forward knee:

$$\mathbf{p}_d(t) = [x_{id}(t) \quad y_{id}(t)]^T = \mathbf{p}_{Fd}(t) - \mathbf{p}_{Hd}(t) \quad (4a)$$

$$\mathbf{p}_d(t) = \Psi[\Theta_d(t)] \Rightarrow \Theta_d(t) = \Psi^{-1}[\mathbf{p}_d(t)] \quad (4b)$$

$$\dot{\Theta}_d(t) = \mathbf{J}^{-1}[\dot{\mathbf{p}}_d(t)], \quad \mathbf{J} = \frac{\partial \Psi}{\partial \Theta_d} \quad (4c)$$

### III. ROBOT DYNAMICS AND CONTROL ARCHITECTURE

#### A. Inverse Dynamics Computation

The model for the robot inverse dynamics is formulated as:

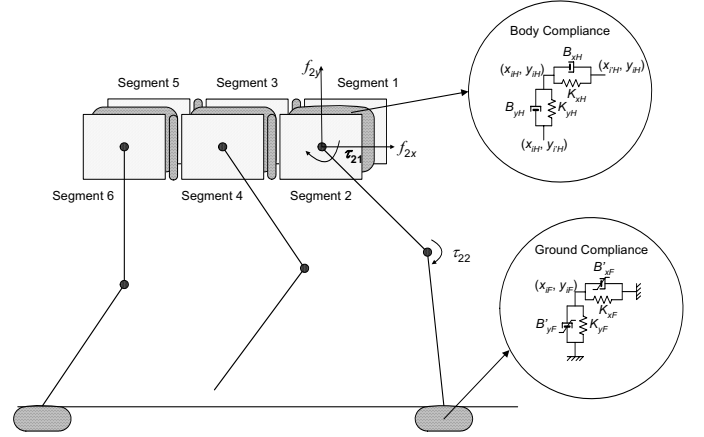


Fig. 2. Model of the robot body and foot-ground interaction.

$$\Gamma = \mathbf{H}(\Theta)\ddot{\Theta} + \mathbf{c}(\Theta, \dot{\Theta}) + \mathbf{g}(\Theta) - \mathbf{F}_{RH} - \mathbf{J}_F^T(\Theta)\mathbf{F}_{RF} \quad (5)$$

where  $\Gamma = [f_{ix}, f_{iy}, \tau_{i1}, \tau_{i2}]^T$  ( $i = 1, \dots, n$ ) is the vector of forces / torques,  $\Theta = [x_{iH}, y_{iH}, \theta_{i1}, \theta_{i2}]^T$  is the vector of position coordinates,  $\mathbf{H}(\Theta)$  is the inertia matrix and  $\mathbf{c}(\Theta, \dot{\Theta})$  and  $\mathbf{g}(\Theta)$  are the vectors of centrifugal / Coriolis and gravitational forces / torques, respectively. The  $n \times m$  ( $m = 2$ ) matrix  $\mathbf{J}_F^T(\Theta)$  is the transpose of the robot Jacobian matrix,  $\mathbf{F}_{RH}$  is the  $m \times 1$  vector of the body inter-segment forces and  $\mathbf{F}_{RF}$  is the  $m \times 1$  vector of the reaction forces that the ground exerts on the robot feet. These forces are null during the foot transfer phase. During the system simulation, Eq. (5) is integrated through the Runge-Kutta method.

We consider that the joint actuators are not ideal, exhibiting a saturation given by:

$$\tau_{ijm} = \begin{cases} \tau_{ijC} & , |\tau_{ijm}| \leq \tau_{ijMax} \\ \text{sgn}(\tau_{ijC}) \cdot \tau_{ijMax} & , |\tau_{ijm}| > \tau_{ijMax} \end{cases} \quad (6)$$

where, for leg  $i$  and joint  $j$ ,  $\tau_{ijC}$  is the controller demanded torque,  $\tau_{ijMax}$  is the maximum torque that the actuator can supply and  $\tau_{ijm}$  is the motor effective torque.

#### B. Robot Body Model

Figure 2 presents the dynamic model for the hexapod body and foot-ground interaction. It is considered robot body compliance because most walking animals have a spine that allows supporting the locomotion with improved stability. In the present study, the robot body is divided in  $n$  identical segments (each with mass  $M_b n^{-1}$ ) and a linear spring-damper system is adopted to implement the intra-body compliance according to:

$$f_{\eta H} = \sum_{i=1}^u [-K_{\eta H}(\eta_{iH} - \eta_{i+1H}) - B_{\eta H}(\dot{\eta}_{iH} - \dot{\eta}_{i+1H})] \quad (7)$$

where  $(x_{iH}, y_{iH})$  are the hip coordinates and  $u$  is the total number of segments adjacent to leg  $i$ .

In this study, the parameters  $K_{\eta H}$  and  $B_{\eta H}$  ( $\eta = \{x, y\}$ ) in the {horizontal, vertical} directions, respectively, are defined so that the body behaviour is similar to the one expected to occur on an animal (Table I).

### C. Foot-Ground Interaction Model

The contact of the  $i^{\text{th}}$  robot feet with the ground is modelled through a non-linear system [3, 4] with linear stiffness  $K_{\eta F}$  and non-linear damping  $B_{\eta F}$  ( $\eta = \{x, y\}$ ) in the {horizontal, vertical} directions, respectively (see Fig. 2), yielding:

$$\begin{aligned} f_{i\eta F} &= -K_{\eta F}(\eta_{iF} - \eta_{iF0}) - B_{\eta F} [-(y_{iF} - y_{iF0})]^{v_\eta} (\dot{\eta}_{iF} - \dot{\eta}_{iF0}) \\ v_x &= 1.0, v_y = 0.9 \end{aligned} \quad (8)$$

where  $x_{iF0}$  and  $y_{iF0}$  are the coordinates of foot  $i$  touchdown and  $v_\eta$  ( $\eta = \{x, y\}$ ) is a parameter dependent on the ground characteristics. The values for the parameters  $K_{\eta F}$  and  $B_{\eta F}$  (Table I) are based on the studies of soil mechanics [4].

### D. Control Architecture

The general control architecture of the hexapod robot is presented in Fig. 3. In the control architecture implemented for this simulation model, the trajectory planning is carried out in the cartesian space but the control is performed in the joint space, which requires the integration of the inverse kinematic model in the forward path. The control algorithm includes an external position feedback loop and an internal loop with information of the foot-ground interaction force.

On a previous work were demonstrated the advantages of this cascade controller, with PD position control and foot force feedback, over a classical PD with, merely, position feedback, particularly in real situations where we have non-ideal actuators with saturation and being also more robust for variable ground characteristics [4].

On a previous work were demonstrated the advantages of this cascade controller, with PD position control and foot force feedback, over a classical PD with, merely, position feedback, particularly in real situations where we have non-ideal actuators with saturation and being also more robust for variable ground characteristics [4].

Previous studies have also allowed us to conclude that the control of a hexapod walking robot through a FO PD $^\alpha$  algorithm guaranteed the best performance for the fractional order  $\alpha_j = 0.5$  [1].

Based on these results, for  $G_{c1}(s)$  we adopt a FO PD $^\alpha$  controller ( $\alpha_j = 0.5$ ), while for  $G_{c2}$  is considered a simple P controller with gain  $Kp_j = 0.9$  ( $j = 1, 2$ ). For the FO PD $^\alpha$  algorithm we have, for joint  $j$ :

$$G_{C1j}(s) = Kp_j + K\alpha_j s^{\alpha_j}, \quad \alpha_j \in \mathfrak{R}, \quad j = 1, 2 \quad (9)$$

where  $Kp_j$  and  $K\alpha_j$  are the proportional and derivative gains, respectively, and  $\alpha_j$  is the fractional order, for joint  $j$ .

For implementing the FO algorithm (Eq. (9)) different approaches can be adopted. It is possible to consider a discrete-time  $u^{\text{th}}$  order Padé approximation ( $a_{ij}, b_{ij} \in \mathfrak{R}$ ,  $j = 1, 2$ ) yielding an equation in the  $z$ -domain of the type:

$$G_{C1j}(z) \approx Kp_j + K\alpha_j \sum_{i=0}^{i=u} a_{ij} z^{-i} / \sum_{i=0}^{i=u} b_{ij} z^{-i} \quad (10)$$

Alternatively, the FO algorithm can be approximated by a truncated series of  $v$  terms according to:

$$D^\alpha f(t) \approx \frac{1}{T^\alpha} \sum_{k=0}^v \zeta_k^\alpha f(t - kT) \quad (11)$$

TABLE I

SYSTEM PARAMETERS

Robot model parameters		Locomotion parameters	
$S_P$	1 m	$\beta$	50%
$L_{ij}, j=1,2$	0.5 m	$L_S$	1 m
$O_i$	0 m	$H_B$	0.9 m
$M_b$	88.0 kg	$F_C$	0.1 m
$M_{ij}, j=1,2$	1 kg	$V_F$	1 ms $^{-1}$
$K_{xH}$	10 $^5$ Nm $^{-1}$	<b>Ground parameters</b>	
$K_{yH}$	10 $^4$ Nm $^{-1}$	$K_{x_F}$	1.3 $\times$ 10 $^6$ Nm $^{-1}$
$B_{xH}$	10 $^3$ Nsm $^{-1}$	$K_{y_F}$	1.7 $\times$ 10 $^6$ Nm $^{-1}$
$B_{yH}$	10 $^2$ Nsm $^{-1}$	$B_{x_F}$	2.3 $\times$ 10 $^6$ Nsm $^{-1}$
		$B_{y_F}$	2.7 $\times$ 10 $^6$ Nsm $^{-1}$

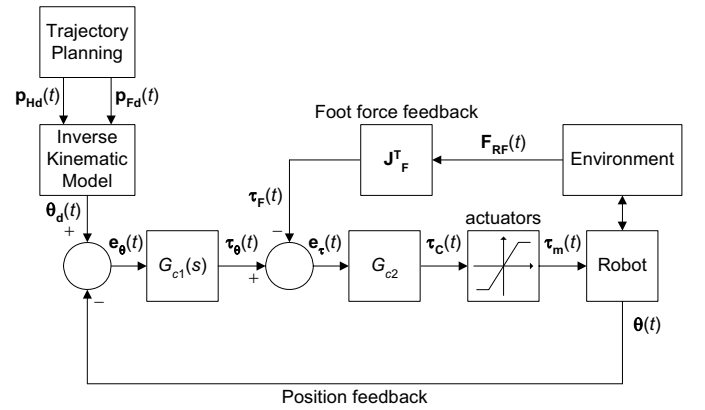


Fig. 3. Hexapod robot control architecture.

where the series coefficients can be calculated iteratively using the expression:

$$\zeta_0^\alpha = 1 \mapsto \zeta_k^\alpha = \left(1 - \frac{\alpha+1}{k}\right) \zeta_{k-1}^\alpha, \quad k = 1, 2, 3, \dots \quad (12)$$

Considering this, the present study evaluates and compares the performance of Fractional Order Proportional and Derivative (FO PD $^{0.5}$ ) control algorithm implementations using the two above mentioned approximations and different number of terms. The analysis is based on two indices introduced in the next section.

## IV. MEASURES FOR PERFORMANCE EVALUATION

In mathematical terms we establish two global measures of the overall performance of the mechanism in an average sense. In this perspective, we define one index  $\{E_{av}\}$  inspired on the system dynamics and another one  $\{\varepsilon_{xyH}\}$  based on the trajectory tracking errors.

Regarding the mean absolute density of energy per travelled distance  $E_{av}$ , it is computed assuming that energy regeneration is not available by actuators doing negative work (by taking the absolute value of the power). At a given joint  $j$  (each leg has  $m = 2$  joints) and leg  $i$  (since we are adopting a hexapod it yields  $n = 6$  legs), the mechanical power is the product of the motor torque and angular velocity. The global index  $E_{av}$  is obtained by averaging the mechanical absolute energy delivered over the travelled distance  $d$ :

$$E_{av} = \frac{1}{d} \sum_{i=1}^n \sum_{j=1}^m \int_0^T |\tau_{ij}(t) \dot{\theta}_{ij}(t)| dt \quad [\text{Jm}^{-1}] \quad (13)$$

In what concerns the hip trajectory following errors we define the index:

$$\varepsilon_{xyH} = \sum_{i=1}^n \sqrt{\frac{1}{N_s} \sum_{k=1}^{N_s} (\Delta_{ixH}^2 + \Delta_{iyH}^2)} \quad [\text{m}] \quad (14)$$

$$\Delta_{ixH} = x_{iHd}(k) - x_{iH}(k), \Delta_{iyH} = y_{iHd}(k) - y_{iH}(k)$$

where  $N_s$  is the total number of samples for averaging purposes and  $\{d, r\}$  indicate the  $i^{\text{th}}$  samples of the desired and real position, respectively.

In all cases the performance optimization requires the minimization of each index.

## V. SIMULATION RESULTS

### A. Simulation Parameters and Controller Tuning

In this section we develop a set of simulations to analyse the performances of the FO PD<sup>0.5</sup>  $G_{c1}(s)$  control algorithm implementations using the two above mentioned approximations and different number of terms, during a periodic wave gait at a constant forward velocity  $V_F$ . For simulation purposes we consider the locomotion parameters, the robot body parameters and the ground parameters (supposing that the robot is walking on a ground of compact clay) presented in Table I.

To tune the different controller implementations we adopt a systematic method, testing and evaluating a narrow grid of several possible combinations of parameters, for all controller implementations. Namely, we vary the controller gains in the intervals  $0.0 \leq Kp_j \leq 10^5$  and  $0.0 \leq K\alpha_j \leq 10^5$ , while assuming high performance joint actuators (maximum actuator torque in Eq. (6) of  $\tau_{ij\text{Max}} = 400 \text{ Nm}$ ) and a  $G_{c2}$  controller with gain  $Kp_j = 0.9$  ( $j = 1, 2$ ).

We start by considering the Padé approximation for the implementation of the  $G_{c1}(s)$  control algorithm. For this case we tune the FO PD<sup>0.5</sup> joint controllers for different orders  $u$  of the Padé ( $0 \leq u \leq 15$  and  $u = \{20, 25\}$ ). Afterwards, we consider the series approximation for the implementation of the  $G_{c1}(s)$  control algorithm, and we repeat the controller tuning procedure for different number of terms  $v$  of the series ( $0 \leq v \leq 10$  and  $v = \{15, 20, 25, 30, 35, 40, 45, 50, 55, 60, 65, 70, 75, 80, 85, 90, 95, 100\}$ ). The controller tuning results, for both cases, are presented in Tables II – VII.

### B. Padé Approximation

Each dot in the charts of Figure 4 depicts the results of a particular  $G_{c1}(s)$  controller tuning ( $\{Kp_j, K\alpha_j\}$ ), in terms of  $\{\varepsilon_{xyH}, E_{av}\}$  for different orders  $u$  ( $u = \{1, 2, 4, 6, 13\}$ ) of the Padé approximation.

We conclude that for the orders  $u = 0$  and  $u > 14$  there is no  $G_{c1}(s)$  controller tuning that allows the locomotion to be performed with the performance measures on the ranges  $0.5 \leq \varepsilon_{xyH} \leq 3.0$  and  $350.0 \leq E_{av} \leq 600.0$ . For values such that

$1 \leq u \leq 13$  we have several different tunings allowing the locomotion to be performed inside these performance measures ranges.

From the observation of Figure 4, it is concluded that for the Padé order  $u = 1$  there is no  $G_{c1}(s)$  controller tuning that allows the locomotion to be performed with simultaneous low hip trajectory tracking errors ( $\varepsilon_{xyH} \leq 1.0$ ) and low energy consumption ( $E_{av} \leq 400.0$ ).

For increasing orders  $u$ , the number of possible  $G_{c1}(s)$  controller tuning, that allows the locomotion to be performed with simultaneous low values for  $\varepsilon_{xyH}$  and  $E_{av}$ , increases until  $u \approx 6$ . For higher Padé orders  $7 \leq u \leq 13$  this number starts to decrease again. Finally, as previously stated, for  $u \approx 14$  the number of “good” solutions becomes zero.

This first analysis, based solely on the possible number of “good” solutions, might lead us to state that, for this application of the PD<sup>0.5</sup> controller, it is best to use a Padé approximation with  $3 \leq u \leq 6$ . In the sequel we are going to analyse the best solution when it is chosen taking into account only the minimization of the performance measure  $\varepsilon_{xyH}$ , only the minimization of the index  $E_{av}$  or a compromise for the simultaneous minimization of  $\varepsilon_{xyH}$  and  $E_{av}$ .

Table II presents the best  $G_{c1}(s)$  controller tuning for different orders of the Padé approximation, when considering the best solution as the one that presents the minimum value of  $\varepsilon_{xyH}$ . We conclude that the best solution corresponds to the Padé order  $u = 4$ , followed by the Padé orders  $u = 3$  and  $u = 5$ . Moreover, for  $2 \leq u \leq 13$  the results remain very similar, both in terms of  $\varepsilon_{xyH}$  and  $E_{av}$ .

Following we analyse the best  $G_{c1}(s)$  controller tuning for different values of  $u$ , when considering the best solution as the one that presents the minimum value of  $E_{av}$ . We conclude, from the analysis of Table III, that the best solution corresponds to the Padé order  $u = 13$ . From the observation of the same table, we conclude that for  $2 \leq u \leq 13$  the results remain very similar, both in terms of  $\varepsilon_{xyH}$  and  $E_{av}$ .

Finally, we analyse the best locomotion performance, for distinct values  $u$  of the Padé approximation for the  $G_{c1}(s)$  control algorithm, while considering that the best solution corresponds to a compromise between the simultaneous minimization of  $\varepsilon_{xyH}$  and  $E_{av}$ . From this viewpoint, we conclude that the best solutions correspond to the Padé orders  $3 \leq u \leq 9$  (Table IV). Outside these values there is a clear degradation of the hexapod locomotion performance, more pronounced for the Padé approximations of orders  $u = 0$  and  $u = 14$ .

It is worth mentioning that another criterion to be considered when choosing the Padé order for a practical implementation is the required computation power. From this viewpoint, low order Padé approximations are preferred. Therefore, and considering all the previous results, we may state that the best order for the Padé approximation when computing the  $G_{c1}(s)$  algorithm yields for  $u \approx 4$ .

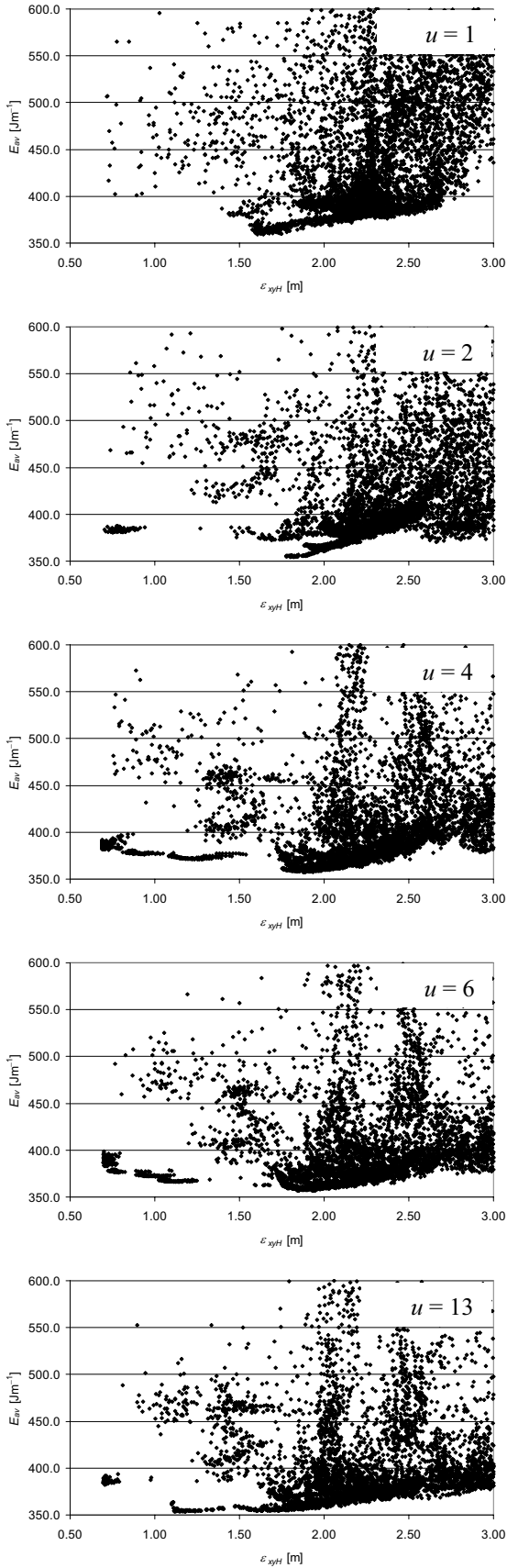


Fig. 4. Plots of  $\epsilon_{xyH}$  vs.  $E_{av}$  for different orders ( $u = \{1, 2, 4, 6, 13\}$ ) of the Padé approximation for the  $PD^{0.5} G_{c1}(s)$  controller, with  $G_{c2} = 0.9$ .

TABLE II

MINIMUM VALUES OF  $\epsilon_{xyH}$ , AND THE CORRESPONDING VALUES OF  $E_{av}$ , FOR DIFFERENT ORDERS  $u$  OF THE PADÉ APPROXIMATION FOR THE  $PD^{0.5} G_{c1}(s)$  CONTROLLER, WITH  $G_{c2} = 0.9$

$u$	$\epsilon_{xyH}$	$E_{av}$	$Kp_1$	$Kp_2$	$K\alpha_1$	$K\alpha_2$
0	1.647	2210.305	4000.0	1000.0	0.0	0.0
1	0.718	506.752	9000.0	5000.0	4500.0	0.0
2	0.703	383.916	10000.0	4000.0	9500.0	0.0
3	0.692	380.852	10000.0	1000.0	8000.0	500.0
4	0.688	390.432	6000.0	2000.0	10000.0	500.0
5	0.695	386.954	7000.0	4000.0	9500.0	0.0
6	0.696	395.448	10000.0	4000.0	9500.0	0.0
7	0.696	386.657	10000.0	4000.0	9500.0	0.0
8	0.696	395.305	6000.0	4000.0	9000.0	0.0
9	0.697	386.919	5000.0	4000.0	9000.0	0.0
10	0.697	387.293	5000.0	4000.0	9000.0	0.0
11	0.697	389.391	7000.0	4000.0	9000.0	0.0
12	0.697	387.966	7000.0	4000.0	9000.0	0.0
13	0.697	384.518	10000.0	4000.0	9000.0	0.0
14	2.342	896.129	3000.0	1000.0	0.0	0.0

TABLE III

MINIMUM VALUES OF  $E_{av}$ , AND THE CORRESPONDING VALUES OF  $\epsilon_{xyH}$ , FOR DIFFERENT ORDERS  $u$  OF THE PADÉ APPROXIMATION FOR THE  $PD^{0.5} G_{c1}(s)$  CONTROLLER, WITH  $G_{c2} = 0.9$

$u$	$\epsilon_{xyH}$	$E_{av}$	$Kp_1$	$Kp_2$	$K\alpha_1$	$K\alpha_2$
0	2.342	896.129	3000.0	1000.0	0.0	0.0
1	1.605	359.444	1000.0	1000.0	9500.0	500.0
2	1.801	354.620	9000.0	1000.0	9000.0	500.0
3	1.854	356.922	5000.0	2000.0	8000.0	500.0
4	1.874	357.603	10000.0	3000.0	7000.0	500.0
5	1.782	357.604	0.0	2000.0	6500.0	500.0
6	1.852	356.767	0.0	2000.0	6500.0	500.0
7	1.823	355.104	0.0	0.0	5500.0	500.0
8	1.683	354.495	5000.0	0.0	6000.0	500.0
9	1.509	354.469	2000.0	0.0	7000.0	500.0
10	1.772	354.338	0.0	1000.0	6500.0	500.0
11	1.752	354.901	0.0	1000.0	6500.0	500.0
12	1.729	354.844	5000.0	2000.0	7000.0	500.0
13	1.182	353.694	0.0	0.0	7500.0	500.0
14	3.292	1051.539	5000.0	1000.0	0.0	0.0

TABLE IV

BEST COMPROMISE SITUATION IN TERMS OF THE SIMULTANEOUS MINIMIZATION OF  $\epsilon_{xyH}$  AND  $E_{av}$ , FOR DIFFERENT ORDERS  $u$  OF THE PADÉ APPROXIMATION FOR THE  $PD^{0.5} G_{c1}(s)$  CONTROLLER, WITH  $G_{c2} = 0.9$

$u$	$\epsilon_{xyH}$	$E_{av}$	$Kp_1$	$Kp_2$	$K\alpha_1$	$K\alpha_2$
0	2.342	896.129	3000.0	1000.0	0.0	0.0
1	0.765	402.417	0.0	4000.0	10000.0	0.0
2	0.712	381.752	8000.0	4000.0	9500.0	0.0
3	0.705	378.329	9000.0	1000.0	7000.0	500.0
4	0.693	381.761	7000.0	2000.0	6500.0	500.0
5	0.700	379.140	10000.0	2000.0	7500.0	500.0
6	0.723	378.022	5000.0	2000.0	7500.0	500.0
7	0.718	378.770	10000.0	2000.0	7500.0	500.0
8	0.773	369.837	3000.0	0.0	10000.0	500.0
9	0.753	369.331	3000.0	0.0	7500.0	500.0
10	0.726	375.215	8000.0	1000.0	8000.0	500.0
11	0.720	374.603	0.0	1000.0	7500.0	500.0
12	0.722	374.091	0.0	1000.0	7000.0	500.0
13	0.703	382.705	3000.0	4000.0	9000.0	0.0
14	2.342	896.129	3000.0	1000.0	0.0	0.0

### C. Series Approximation

Such as in the charts of Figure 4, each dot in the charts of Figure 5 depicts the results of a particular  $G_{c1}(s)$  controller tuning ( $\{Kp_j, K\alpha_j\}$ ), in terms of  $\{\varepsilon_{xyH}, E_{av}\}$  for different number of terms  $\nu$  ( $\nu = \{20, 40, 60, 80, 100\}$ ) of the Series approximation. From the observation of this Figure, it is concluded that for all tested number of terms  $\nu$  of the Series approximation, the number of possible  $G_{c1}(s)$  controller tuning, that allows the locomotion to be performed inside the interval  $\varepsilon_{xyH} \leq 3.0$  and  $E_{av} \leq 400.0$ , remains approximately the same. Furthermore, we observe that as the number of terms  $\nu$  of the Series approximation increases, the best compromise  $G_{c1}(s)$  controller tuning, in terms of the simultaneous minimization of  $\varepsilon_{xyH}$  and  $E_{av}$ , presents smaller values of the index  $E_{av}$  but at the cost of higher values of  $\varepsilon_{xyH}$ .

Finally, we conclude that for all tested number of terms  $\nu$  of the Series approximation there is no  $G_{c1}(s)$  controller tuning that allows the locomotion to be performed with simultaneous low hip trajectory tracking errors ( $\varepsilon_{xyH} \leq 1.0$ ) and low energy consumption ( $E_{av} \leq 400.0$ ), as was the case for the orders  $2 \leq u \leq 13$ , when considering the Padé approximation.

Therefore, we conclude that with the Series approximation for the implementation of the FO PD<sup>0.5</sup>  $G_{c1}(s)$  controller, for the number of terms tested, we can never reach the same performance as with the Padé approximation.

As in the case of the Padé approximation, this first analysis was based solely on the possible number of “good” solutions. In the sequel we are going to analyse the best solution when it is chosen taking into account only the minimization of the performance measure  $\varepsilon_{xyH}$ , only the minimization of the index  $E_{av}$  or a compromise for the simultaneous minimization of  $\varepsilon_{xyH}$  and  $E_{av}$ .

Table V presents the best  $G_{c1}(s)$  controller tuning for different number of terms of the Series, when considering the best solution as the one that presents the minimum value of  $\varepsilon_{xyH}$ . We conclude that the best solution corresponds to the Series approximation with only one term ( $\nu = 1$ ), but at the cost of a high value for  $E_{av}$ , followed by the Series approximations with small number of terms ( $\nu = 2$  and  $\nu = 3$ ). Moreover, for  $4 \leq \nu \leq 100$  the results do not present a significant change in terms of  $\varepsilon_{xyH}$ .

Following we analyse the best  $G_{c1}(s)$  controller tuning for different values of  $\nu$ , when considering the best solution as the one that presents the minimum value of  $E_{av}$ . We conclude, from the analysis of Table VI, that the best solution corresponds to a Series with  $\nu = 5$  terms. From the observation of the same table, we conclude that for  $4 \leq \nu \leq 8$  the results remain very similar, both in terms of  $\varepsilon_{xyH}$  and  $E_{av}$ .

Finally, we analyse the best locomotion performance, for distinct values  $\nu$  of the Series approximation for the  $G_{c1}(s)$  control algorithm, while considering that the best solution corresponds to a compromise between the simultaneous minimization of  $\varepsilon_{xyH}$  and  $E_{av}$ . From this viewpoint, we conclude that the best solutions correspond to a Series approximation with  $55 \leq \nu \leq 60$  (Table VII). Outside these values of  $\nu$ , the hexapod locomotion performance is only slightly inferior.

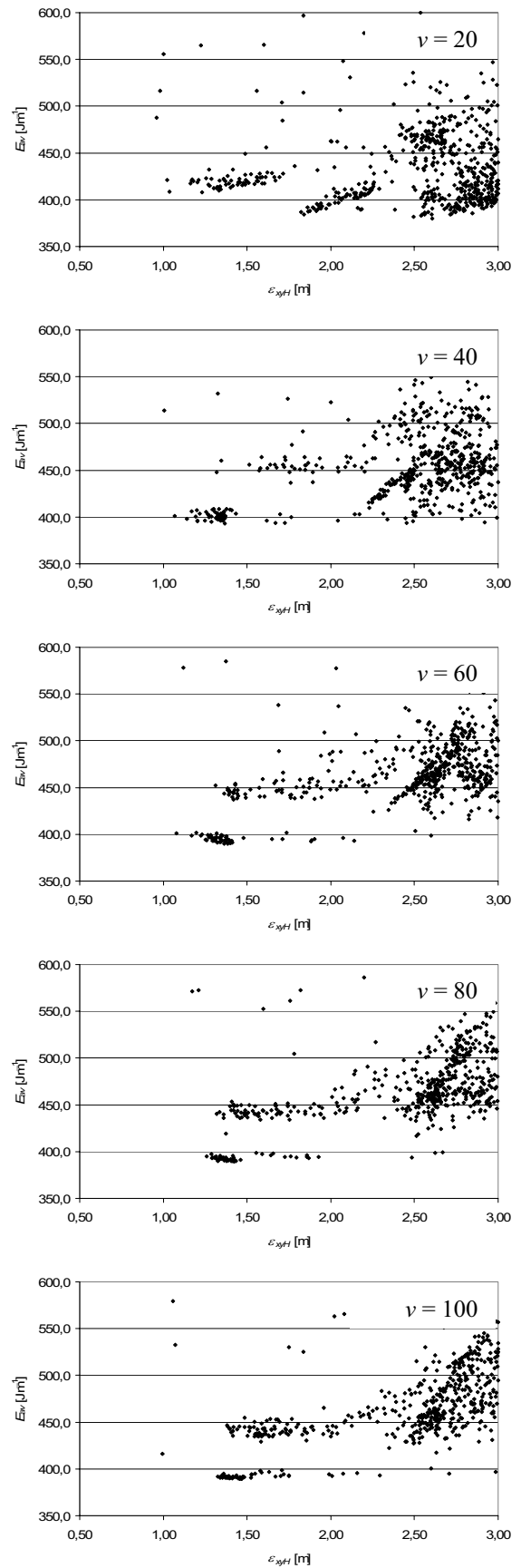


Fig. 5. Plots of  $\varepsilon_{xyH}$  vs.  $E_{av}$  for different number of terms ( $\nu = \{20, 40, 60, 80, 100\}$ ) of the Series approximation for the PD<sup>0.5</sup>  $G_{c1}(s)$  controller, with  $G_{c2} = 0.9$ .



TABLE V

MINIMUM VALUES OF  $\varepsilon_{xyH}$ , AND THE CORRESPONDING VALUES OF  $E_{av}$ , FOR DIFFERENT NUMBER OF TERMS  $\nu$  OF THE SERIES APPROXIMATION FOR THE PD<sup>0.5</sup>  $G_{c1}(s)$  CONTROLLER, WITH  $G_{c2} = 0.9$

$\nu$	$\varepsilon_{xyH}$	$E_{av}$	$Kp_1$	$Kp_2$	$K\alpha_1$	$K\alpha_2$
1	0,683	3396,917	8000,0	10000,0	10000,0	0,0
2	0,723	510,658	1000,0	5000,0	6000,0	0,0
3	0,709	466,276	6000,0	5000,0	6000,0	0,0
4	0,901	633,294	10000,0	1000,0	1500,0	0,0
5	0,975	584,126	2000,0	2000,0	1000,0	0,0
6	0,905	1231,619	5000,0	8000,0	1500,0	0,0
7	0,915	460,399	1000,0	3000,0	7000,0	0,0
8	0,950	454,061	2000,0	3000,0	7000,0	0,0
9	0,984	452,685	5000,0	3000,0	7000,0	0,0
10	0,937	608,086	7000,0	2000,0	1000,0	0,0
15	0,997	424,532	1000,0	3000,0	7500,0	0,0
20	0,959	487,575	5000,0	3000,0	1000,0	0,0
25	0,991	1080,407	9000,0	9000,0	1500,0	0,0
30	0,987	559,462	9000,0	2000,0	1000,0	0,0
35	1,010	569,030	9000,0	2000,0	1000,0	0,0
40	1,005	514,262	8000,0	2000,0	500,0	0,0
45	0,998	700,988	6000,0	6000,0	1000,0	0,0
50	1,054	403,158	7000,0	3000,0	7500,0	0,0
55	0,982	2232,976	0,0	7000,0	1000,0	0,0
60	1,025	683,768	8000,0	3000,0	500,0	0,0
65	0,968	529,101	5000,0	1000,0	500,0	0,0
70	1,137	623,160	5000,0	1000,0	500,0	0,0
75	0,949	497,731	9000,0	1000,0	1000,0	0,0
80	1,046	1749,605	0,0	7000,0	1000,0	0,0
85	0,978	571,619	9000,0	3000,0	500,0	0,0
90	0,974	438,394	0,0	1000,0	1000,0	0,0
95	0,905	417,806	0,0	1000,0	1000,0	0,0
100	0,995	416,099	0,0	1000,0	1000,0	0,0

TABLE VI

MINIMUM VALUES OF  $E_{av}$ , AND THE CORRESPONDING VALUES OF  $\varepsilon_{xyH}$ , FOR DIFFERENT NUMBER OF TERMS  $\nu$  OF THE SERIES APPROXIMATION FOR THE PD<sup>0.5</sup>  $G_{c1}(s)$  CONTROLLER, WITH  $G_{c2} = 0.9$

$\nu$	$\varepsilon_{xyH}$	$E_{av}$	$Kp_1$	$Kp_2$	$K\alpha_1$	$K\alpha_2$
1	2,192	481,299	7000,0	1000,0	10000,0	0,0
2	1,337	411,955	0,0	9000,0	8000,0	0,0
3	1,468	381,030	0,0	9000,0	9500,0	0,0
4	1,846	376,568	5000,0	10000,0	9000,0	0,0
5	1,781	375,136	0,0	10000,0	10000,0	0,0
6	1,937	376,028	3000,0	10000,0	10000,0	0,0
7	1,885	375,787	9000,0	10000,0	10000,0	0,0
8	1,956	375,458	10000,0	10000,0	10000,0	0,0
9	2,011	385,535	9000,0	10000,0	10000,0	0,0
10	3,060	383,653	3000,0	7000,0	8500,0	0,0
15	2,139	381,671	5000,0	7000,0	8500,0	0,0
20	2,608	379,670	10000,0	8000,0	8000,0	0,0
25	2,492	384,839	10000,0	8000,0	8500,0	0,0
30	3,108	386,714	1000,0	10000,0	9000,0	0,0
35	3,324	388,081	1000,0	10000,0	8500,0	0,0
40	3,326	384,905	0,0	9000,0	8000,0	0,0
45	3,320	383,168	4000,0	8000,0	8000,0	0,0
50	3,450	383,338	0,0	9000,0	7500,0	0,0
55	3,557	380,838	0,0	8000,0	7000,0	0,0
60	3,550	381,108	1000,0	8000,0	7000,0	0,0
65	3,433	382,038	6000,0	8000,0	7500,0	0,0
70	3,625	381,282	3000,0	7000,0	6500,0	0,0
75	3,432	382,868	4000,0	8000,0	7000,0	0,0
80	3,469	381,015	10000,0	7000,0	6500,0	0,0
85	3,451	382,036	9000,0	9000,0	7500,0	0,0
90	3,499	382,608	9000,0	8000,0	7000,0	0,0
95	3,744	382,258	4000,0	8000,0	6500,0	0,0
100	3,579	383,197	9000,0	8000,0	7000,0	0,0

TABLE VII

BEST COMPROMISE SITUATION IN TERMS OF THE SIMULTANEOUS MINIMIZATION OF  $\varepsilon_{xyH}$  AND  $E_{av}$ , FOR DIFFERENT NUMBER OF TERMS  $\nu$  OF THE SERIES APPROXIMATION FOR THE PD<sup>0.5</sup>  $G_{c1}(s)$  CONTROLLER, WITH  $G_{c2} = 0.9$

$\nu$	$\varepsilon_{xyH}$	$E_{av}$	$Kp_1$	$Kp_2$	$K\alpha_1$	$K\alpha_2$
1	1,536	483,682	2000,0	1000,0	10000,0	0,0
2	1,337	411,955	0,0	9000,0	8000,0	0,0
3	1,399	390,170	6000,0	9000,0	9500,0	0,0
4	1,002	425,485	7000,0	4000,0	10000,0	0,0
5	1,520	383,729	7000,0	9000,0	10000,0	0,0
6	1,557	380,792	10000,0	9000,0	10000,0	0,0
7	1,441	392,526	1000,0	6000,0	9500,0	0,0
8	1,420	395,912	3000,0	6000,0	9000,0	0,0
9	1,471	391,242	7000,0	6000,0	9500,0	0,0
10	1,519	391,600	9000,0	6000,0	9500,0	0,0
15	1,699	384,500	10000,0	6000,0	9500,0	0,0
20	1,839	384,283	10000,0	6000,0	10000,0	0,0
25	1,083	409,884	4000,0	3000,0	7500,0	0,0
30	1,086	401,823	0,0	3000,0	7500,0	0,0
35	1,097	398,280	2000,0	3000,0	7500,0	0,0
40	1,069	401,032	5000,0	3000,0	7500,0	0,0
45	1,124	398,871	5000,0	3000,0	7500,0	0,0
50	1,213	398,301	4000,0	3000,0	8000,0	0,0
55	1,048	398,742	9000,0	3000,0	7500,0	0,0
60	1,076	400,835	10000,0	3000,0	7500,0	0,0
65	1,181	400,856	9000,0	3000,0	7500,0	0,0
70	1,202	399,457	10000,0	3000,0	7500,0	0,0
75	1,193	396,626	10000,0	3000,0	8000,0	0,0
80	1,260	394,820	8000,0	3000,0	8500,0	0,0
85	1,254	395,753	10000,0	3000,0	8500,0	0,0
90	1,313	392,088	6000,0	3000,0	9000,0	0,0
95	1,286	393,259	9000,0	3000,0	8500,0	0,0
100	1,325	391,533	9000,0	3000,0	9500,0	0,0

As can be concluded from the above experiments, the Padé approximation with a small number of terms ( $3 \leq n \leq 6$ ) gives the best results, in terms of simultaneous low values for  $E_{av}$  and  $\varepsilon_{xyH}$ .

#### D. Comparison of the Padé and the Series Approximations

In Figures 6 and 7 are depicted the joint actuation torques  $\tau_{ijm}$  and the hip trajectory tracking errors  $\Delta_{1xH}$  and  $\Delta_{1yH}$ , along one robot locomotion step, considering a 4<sup>th</sup> order ( $u = 4$ ) Padé approximation and a Series approximation with 55 terms ( $\nu = 55$ ) for the PD<sup>0.5</sup>  $G_{c1}(s)$  controller (while assuming the best compromise situation in terms of the simultaneous minimization of  $\varepsilon_{xyH}$  and  $E_{av}$ ) and  $G_{c2} = 0.9$ .

From the analysis of Figure 6 it is possible to conclude that, for the algorithm implementation with this Padé order (according to the previous studies), the joint actuation torques present lower oscillations than for the case of the Series approximation. These oscillations are largely due to the feet impact with the ground at the end of the transfer phase, and are mainly in the hip joint torque being much lower in the knee torque. Furthermore, it is possible to conclude that the torque that the actuators must supply along the locomotion cycle is lower than the actuators saturation torque, as desirable.

Finally, looking into the charts of Figure 7 it is possible to conclude that the errors introduced along the walking robot locomotion cycle are almost negligible in the  $x$  direction, for the case of the Padé approximation, meaning that the controller allows to correctly following the planned trajectory

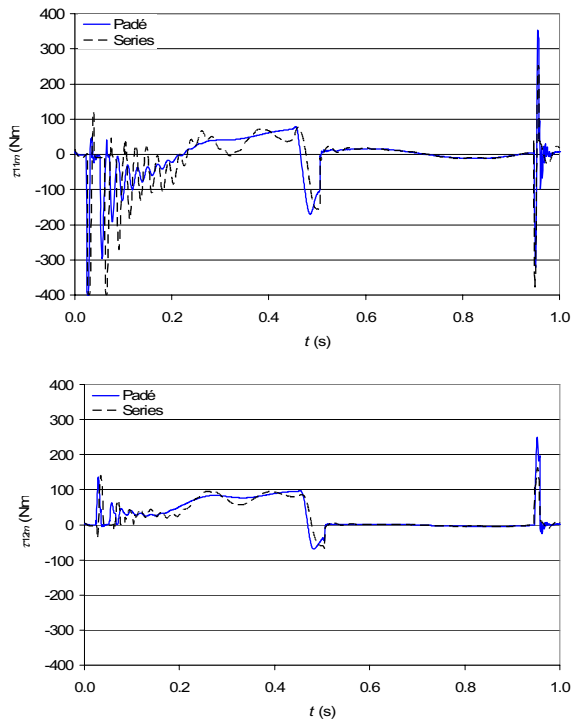


Fig. 6. Plots of  $\tau_{1jm}$  vs.  $t$ , considering a 4<sup>th</sup> order ( $u = 4$ ) Padé approximation and a Series approximation with 55 terms ( $v = 55$ ), while assuming the best compromise situation in terms of the simultaneous minimization of  $\varepsilon_{xyH}$  and  $E_{av}$ , for the  $PD^{0.5} G_{c1}(s)$  controller and  $G_{c2} = 0.9$ .

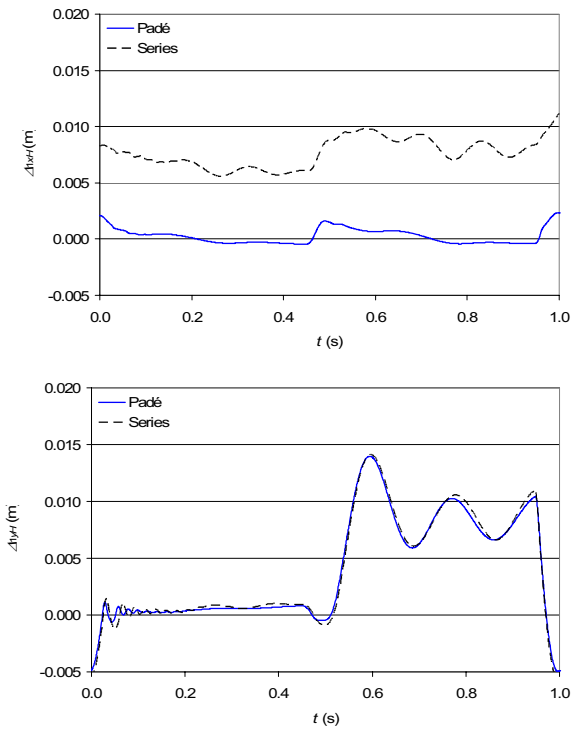


Fig. 7. Plots of  $\Delta_{1xH}$  and  $\Delta_{1yH}$  vs.  $t$ , considering a 4<sup>th</sup> order ( $u = 4$ ) Padé approximation and a Series approximation with 55 terms ( $v = 55$ ), while assuming the best compromise situation in terms of the simultaneous minimization of  $\varepsilon_{xyH}$  and  $E_{av}$ , for the  $PD^{0.5} G_{c1}(s)$  controller and  $G_{c2} = 0.9$ .

being slightly higher for the case of the Series approximation. Along the  $y$  direction, however, it is seen a relatively large trajectory following error during half of the robot locomotion cycle ( $0.5 \leq t \leq 1$  s), for both approximations, that corresponds to the support phase on which the robot has this leg on the ground helping support the robot body. This leads to large efforts on this leg, and correspondingly to the large hip trajectory tracking errors.

## VI. CONCLUSIONS

In this paper we have compared the performance of distinct FO  $PD^{0.5}$  control algorithm implementations (using the Padé and the Series approximations and different number of terms) applied to the leg joint control of a hexapod robot with two dof legs and leg joint actuators having saturation, during a periodic wave gait at a constant forward velocity  $V_F$ .

In order to analyze the system performance two measures were defined, the first based on the mean absolute density of energy per travelled distance and the second on the hip trajectory errors.

The simulation experiments reveal that the  $PD^{0.5}$  controller implementation using the Padé approximation with a small number of terms ( $3 \leq u \leq 6$ ) gives the best results, both in terms of the high possible number of good solutions and in terms of the solution with simultaneous low values for  $E_{av}$  and  $\varepsilon_{xyH}$ .

The focus of the work presented has been on the use of the Padé and the series approximation for the implementation of the  $PD^{0.5}$  controllers with a proportional plus a derivative / integrative term. Future work in this area will also address the study of the performance of a FO PID control algorithm of the type  $PI^2D^\alpha$  and the study of complex-order control algorithms.

## ACKNOWLEDGEMENTS

The first author would like to acknowledge the Financial Support of Fundação Calouste Gulbenkian for his participation in the CLAWAR 2006 Conference.

## REFERENCES

- [1] M. F. Silva and J. A. T. Machado, *Integer vs. Fractional Order Control of a Hexapod Robot, Climbing and Walking Robots*, Manuel A. Armada and Pablo González de Santos (Eds.), Springer, pp. 73–83, 2005.
- [2] M. F. Silva, J. A. T. Machado and R. S. Barbosa, *Complex-Order Dynamics in Hexapod Locomotion*, Signal Processing – Special Section “Fractional Calculus Applications in Signals and Systems”, Vol. 86, Issue 10, pp. 2785 – 2793, 2006.
- [3] M. F. Silva, J. A. T. Machado and A. M. Lopes, *Modelling and Simulation of Artificial Locomotion Systems*, ROBOTICA, **23**, pp. 595 – 606, 2005.
- [4] M. F. Silva, J. A. T. Machado and A. M. Lopes, *Position / Force Control of a Walking Robot*, MIROC –Machine Intelligence and Robot Control, **5**, pp. 33 – 44, 2003.